Carbohydrate Polymers 113 (2014) 388–393

Contents lists available at ScienceDirect

Carbohydrate Polymers

journal homepage: www.elsevier.com/locate/carbpol

Homogeneous isolation of nanocelluloses by controlling the shearing force and pressure in microenvironment

Jihua Li[a,c,*], Yihong Wang[a,b], Xiaoyi Wei[a], Fei Wang[a], Donghui Han[a,b], Qinghuang Wang[a,c], Lingxue Kong[d]

[a] Agriculture Products Processing Research Institute, Chinese Academy of Tropical Agricultural Sciences, Zhanjiang 524001, PR China
[b] College of Food Science and Technology, Huazhong Agricultural University, Wuhan 430070, PR China
[c] National Center of Important Tropical Crops Engineering and Technology Research, Haikou 571101, PR China
[d] Institute for Frontier Materials, Deakin University, Waurn Ponds, Victoria 3216, Australia

ARTICLE INFO

Article history:
Received 1 April 2014
Received in revised form 17 June 2014
Accepted 24 June 2014
Available online 11 July 2014

Keywords:
Dynamic high pressure microfluidization
High pressure homogenization
Homogeneous isolation
Microenvironment
Nanocellulose

Chemical compounds studied in this article:
1-Butyl-3-methylimidazolium chloride (PubChem CID: 2734161)
1-Methylimidazole (PubChem CID: 1390)
1-Chlorobutane (PubChem CID: 8005)
Sodium hydroxide (PubChem CID: 14798)
Nitric acid (PubChem CID: 944)
Potassium bromide (PubChem CID: 253877)
N, N-dimethylacetamide (PubChem CID: 31374)
Lithium chloride (PubChem CID: 433294)
Methanol (PubChem CID: 887)
Sulfuric acid (PubChem CID: 1118)

ABSTRACT

Nanocelluloses were prepared from sugarcane bagasse celluloses by dynamic high pressure microfluidization (DHPM), aiming at achieving a homogeneous isolation through the controlling of shearing force and pressure within a microenvironment. In the DHPM process, the homogeneous cellulose solution passed through chambers at a higher pressure in fewer cycles, compared with the high pressure homogenization (HPH) process. X-ray diffraction (XRD) and X-ray photoelectron spectroscopy (XPS) demonstrated that entangled network structures of celluloses were well dispersed in the microenvironment, which provided proper shearing forces and pressure to fracture the hydrogen bonds. Gel permeation chromatography (GPC), CP/MAS ^{13}C NMR and Fourier transform infrared spectroscopy (FT-IR) measurements suggested that intra-molecular hydrogen bonds were maintained. These nanocelluloses of smaller particle size, good dispersion and lower thermal stability will have great potential to be applied in electronics devices, electrochemistry, medicine, and package and printing industry.

1. Introduction

Celluloses are considered to be a typical kind of biopolymers that are inexhaustible, environmentally friendly and biocompatible to meet the increasing demand for biomaterials (Klemm, Heublein, Fink, & Bohn, 2005) and electronic devices. Due to their extensive hydrogen bonds between polymer backbone and their high crystallinity (Hinterstoisser, Åkerholm, & Salme'n, 2003), the celluloses are chemically stable and insoluble in acidic, alkaline or organic solvents. This high stability presents a challenge for the fine celluloses to be processed and used in a wide range of applications. Therefore, challenges and future opportunities of celluloses will be focused on the processes that can improve the productivity.

Nanocelluloses are normally isolated by means of chemical (Zhang, Ruan, & Zhou, 2001), physical (Ikeda, Holtman, Kadla, Chang, & Jameel, 2002), and biological methods (Lavoine, Desloges, Dufresne, & Bras, 2012). Among them, physical process has been the most widely used method but requires a lot of energy to destroy

* Corresponding author at: Agriculture Products Processing Research Institute, Chinese Academy of Tropical Agricultural Sciences, Zhanjiang, Guangdong 524001, PR China. Tel.: +86 759 2212978; fax: +86 759 2208758.
E-mail address: foodpaper@126.com (J. Li).

http://dx.doi.org/10.1016/j.carbpol.2014.06.085
0144-8617/

the tangles between the molecular chains under solid condition. Recently, ionic liquids have been used as nonderivatizing solvents for the production of celluloses as the extensive hydrogen bonds between cellulose chains can be easily broken by anionic ionic liquids in the homogeneous dissolution process (Swatloski, Spear, Holbrey, & Rogers, 2002). The entangled molecular chain networks are scattered into single molecular chains and form a microenvironment system that facilitates the isolation of nanocelluloses from the dispersed cellulose molecular chains.

In our previous study (Li et al., 2012), the nanocelluloses were successfully prepared with a high pressure homogenization (HPH) process in homogeneous media. Nanocelluloses with a particle size of 10–20 nm were obtained at 80 MPa in 30 cycles. However, the celluloses were degraded to a certain degree during the processing due to too many cycles being used, resulted in the deterioration of materials properties.

Contrary to high pressure homogenization technology, dynamic high pressure microfluidization (DHPM) can produce finer emulsion particles and avoid the occurrence of coalescence or aggregation because of the high shearing force and high stress during the ultra-high pressure homogenization and head-on collision (Hu, Zhao, Sun, Zhao, & Ren, 2011). DHPM has been used to improve the functional properties of peanut proteins, and extend the shelf life of milk (Hu et al., 2011; Pereda, Perragut, Quevedo, Guamis, & Trujillo, 2008) because of the unnoticeable damage to the molecular structures. However, to our knowledge, the DHPM process has not been explored for the fabrication of polymer materials, as the mechanism of the process and its effects on the structure of materials are not well understood.

The objective of this study was to evaluate the effect of homogenization forces on the structural changes of celluloses. In this study, DHPM was applied to isolate nanocelluloses from sugarcane bagasse in a microenvironment. The optimal conditions of the DHPM process were investigated. Compared with the HPH process, the effects of DHPM process were characterized by rheological property, Fourier transform infrared spectroscopy (FT-IR) analysis, X-ray photoelectron spectroscopy, and solid-state CP/MAS ^{13}C NMR.

2. Experimental

2.1. Materials

Sugarcane bagasse was purchased from Guangdong Fengshou Sugar Industry Co., Ltd, Zhanjiang, China, and pretreated by acid and alkali treatment (Adsul, Soni, Bhargava, & Bansal, 2012; Weng, Zhang, Ruan, Shi, & Xu, 2004). Ionic liquid 1-butyl-3-methylimidazolium chloride ([Bmim]Cl) was prepared by following the procedures reported in the literature (Li et al., 2012). All other reagents and chemicals were of analytical grade.

2.2. Preparation of nanocelluloses

Sugarcane bagasse celluloses (SBC) with a content of celluloses up to 93.53% were dissolved in [Bmim]Cl under microwave heating (130 °C, 500 W). They were then homogenized by dynamic high pressure microfluidization (S/N8425, Micro DeBEE Inc., USA) at pressure levels from 34 to 172 MPa and for up to 6 cycles. SBC were precipitated from the ILs solution by water. After that [Bmim]Cl were removed by centrifugal separation. Finally, the regenerated SBC were dried in a vacuum freeze dryer. For comparison purpose, nanocellulose samples treated with high pressure homogenization were also prepared at 80 MPa for 30 cycles under the optimum operating conditions.

2.3. Characterization of supramolecular structures

2.3.1. Particle size distribution

The particle size and size distribution were measured by a photon correlation spectroscopy with a Nano-ZS (Malvern Instruments, UK) in order to characterize the supramolecular structures of the nanocelluloses. The nanocelluloses were diluted in deionized water at pH 7.0 at room temperature. The mean diameter (z-average) was calculated by analyzing the intensity autocorrelation function. The data reported are the average of three replicates.

2.3.2. Morphological analysis

The morphology measurements of the nanocelluloses were carried out on a TEM (JEM-100, JEOL, Tokyo, Japan) operated at 100 keV. The nanocelluloses were deposited from an aqueous dilute dispersion and cast one drop onto copper grid with carbon film support. Samples were observed directly with TEM after they were dried at 20 °C without further staining.

2.3.3. Rheological properties analysis

Dynamic viscoelasticity of celluloses/[Bmim]Cl solution was measured using an AR2000 stress-controlled rheometer (TA Instruments, USA) with 40 mm parallel-plate geometry. The gap chosen was about 1000 μm for all measurements. The experimental temperature was set at 40 °C. The measurements were performed by embedding with a thin layer of standard viscosity silicon oil on the free surface of the solution.

2.3.4. X-ray diffraction (XRD) analysis

X-ray diffractometry in reflection mode were carried out using a diffractometer (Bruker D8 Advance, Germany), with monochromatic Cu Kα radiation (λ = 0.15418 nm), generated at 40 kV and 40 mA, at room temperature. Diffractograms were made by continuous scanning over the range of diffraction angle from 2θ = 5° to 2θ = 45°. Crystallinity index was calculated based on the Segal's empirical method (Sasaki, Adschiri, & Araai, 2003), using the equation:

$$C_{\mathrm{Ir}}(\%) = (I_{2\ 0\ 0} - I_{\mathrm{am}}) \times 100\%/I_{2\ 0\ 0} \quad (1)$$

where I_{200} is the maximum intensity of the principal peak lattice diffraction, and I_{am} is the intensity of diffraction attributed to amorphous celluloses. Integration of crystalline reflection was carried out with Origin Pro software.

2.3.5. X-ray photoelectron spectroscopy (XPS) analysis

XPS measurements were performed to investigate the surface chemical changes of the samples using VG Multilab 2000 (Thermo Electron Corporation, USA) X-ray Photoelectron Spectrometer with Al source. A spot size of 100 μm and a power of 25 W were used. All binding energy values were calculated relative to the carbon (C 1s) photoelectron at 285 eV by applying a linear background subtraction method followed by C 1s curve deconvolution into three Gaussian's curves.

2.3.6. Fourier transform infrared spectroscopy (FT-IR) analysis

The cellulose samples were subjected to Fourier transform infrared (FT-IR) analysis (model: Spectrum GX-1, PerkinElmer, USA spectrometer) to investigate the changes in functional groups. The spectra (4000–400 cm^{-1}) were recorded with a resolution of 1 cm^{-1} and 64 scans per sample. About 2 mg samples were prepared by mixing with 120 mg of spectroscopic grade KBr then compressed to form a disk.

2.3.7. Solid-state CP/MAS ^{13}C NMR analysis

Solid-state ^{13}C NMR spectra were recorded at ambient temperature on an Infinity Plus 400 spectrometer (^{13}C frequency =

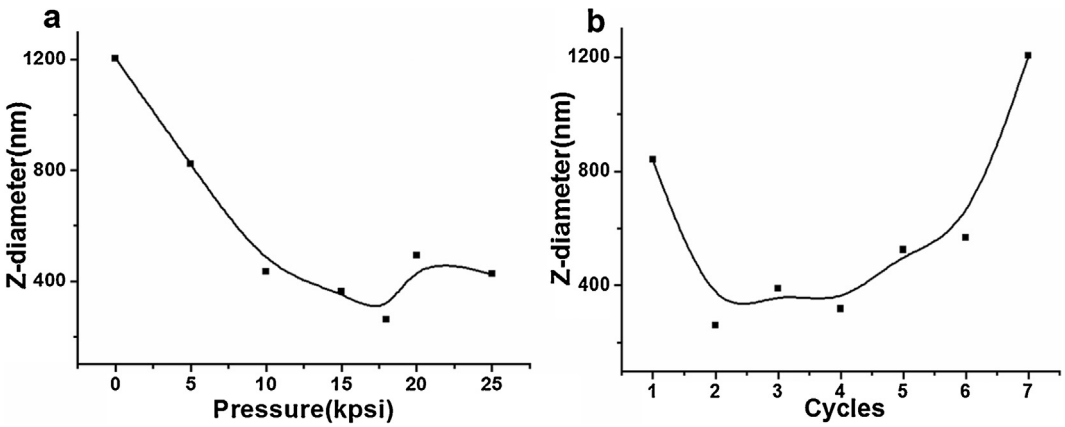

Fig. 1. Particle sizes on different conditions (a, pressure from 34 MPa (5 kpsi) to 172 MPa (25 kpsi) at two cycles; b, operation from one cycle to six cycles at pressure of 124 MPa (18 kpsi)).

100 MHz) with a CP/MAS unit. The spinning was set at a rate of 5000 Hz. The contact time was 1.0 ms, the acquisition time 20.48 ms. Typically, 2000 scans were acquired for each spectrum.

2.3.8. Gel permeation chromatography (GPC) analysis

The gel permeation chromatography (GPC) with manual injector was used which included a G1311B 1260 Quat Pump and a differential refractometer detector (Agilent Technologies, USA). Mobile phases (DMAc/0.5% LiCl) were filtered through a PTFE membrane filter. Separation was performed on a series of two PL gel mixed bed columns (300 × 7.8 mm; particle size 10 μm) at 50 °C, and at the flow rate of 1.0 ml min^{-1}. Eight polystyrene standards of narrow polydispersity were used to calibrate the columns.

2.3.9. Thermal gravimetric (TG) analysis

The thermal stability of the samples was evaluated by thermogravimetry. TG measurements were carried out from 25 °C to 800 °C at a heating rate of 10 °C min^{-1}. All of the measurements were performed under a nitrogen atmosphere with a gas flow of 50 ml min^{-1}.

3. Results and discussion

3.1. Preparation of nanocelluloses by DHPM

When celluloses were dissolved in ionic liquids, hydrogen bond networks of the cellulose chains were dispersed in homogeneous dissolution. During the DHPM process, there are two modes of interaction. The first one is the shearing forces generated from the high pressure homogenization pumps. The other is the pressure from the collision chamber. Therefore, the cellulose structures are determined by the shearing forces and pressure which can be controlled by changing the operating pressure or DHPM times (Martıínez et al., 1997). As can be seen in Fig. 1, the diameter of the nanocelluloses was decreased from 1205 nm to 261 nm with the increase of micro-fluidization pressure or the number of cycles. However, if a higher pressure (more than 124 MPa) or more cycles (more than 2) were used, the mean particle size of the nanocelluloses would become higher due to the droplet coalescence. The polydispersity index remained at a constant value of around 0.3. Therefore, the optimal conditions were two cycles at 124 MPa (18 kpsi) during the whole process.

Fig. 2 shows a TEM micrograph of the nanocelluloses with smallest average diameter under the optimum conditions. TEM analysis of the nanocelluloses provides useful information on the size and morphology of the nanocellulose particles and their status of agglomeration. The nanocellulose particles are spherical in shape with diameters ranging from 5 nm to 12 nm, which is smaller than 10–20 nm for the ones produced with a HPH process (Li et al., 2012). The production of particles with smaller size is largely because of the sudden application of high pressure and the impact from all forces. More interestingly, the nanocellulose particles were well dispersed with no obvious aggregation.

3.2. Effects of DHPM on the structure of nanocellulose

Because of the microenvironment formed by the chambers, a change in shearing force and pressure could have a significant influence on intra-molecular and intermolecular hydrogen bonds of the celluloses. To analyze the effects of these two parameters on the structure and properties of the nanocelluloses, different characterization methods including X-ray diffraction (XRD), X-ray photoelectron spectroscopy (XPS), rheology, Fourier transform infrared spectroscopy (FT-IR), and solid-state CP/MAS ^{13}C NMR were used.

3.2.1. Rheological properties

The viscosity of celluloses/[Bmim]Cl solution treated by DHPM is lower than the one treated by HPH (Fig. 3). This indicates that the entanglement of the cellulose chains was further weakened and the covalent bonds between the celluloses were broken (Collier,

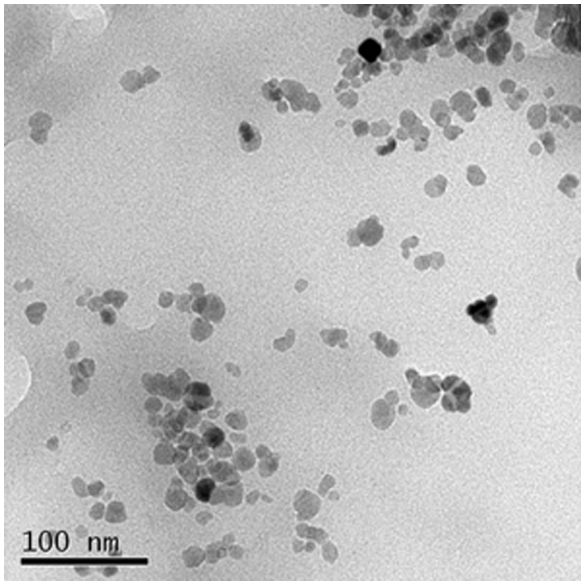

Fig. 2. TEM of nanocelluloses treated with DHPM.

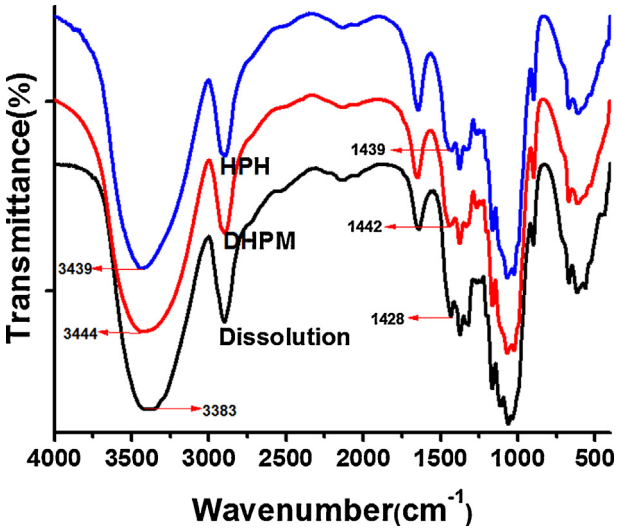

Fig. 3. Rheological properties of celluloses/[Bmim]Cl.

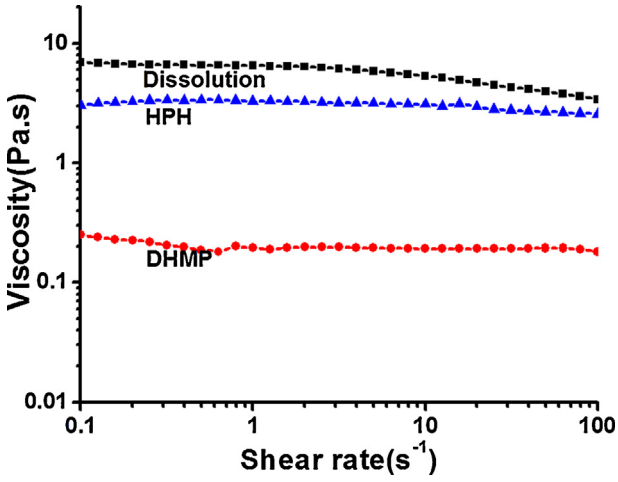

Fig. 4. FT-IR spectra of regenerated celluloses and nanocelluloses treated with DHPM and HPH.

Watson, Collier, & Petrovan, 2009; Weng et al., 2004), due to the ultra-high pressure and higher forces from the high pressure homogenization process pumps and collision chamber in the DHPM process. Therefore, more fractured molecular chains were formed, which also led to significant reduction in the diameter of nanocelluloses.

3.2.2. Crystal structure analysis

The X-ray diffraction patterns showed that the crystal structure presented typical cellulose II for the nanocelluloses treated with both DHPM and HPH (Yue et al., 2012). According to Segal's empirical model (Eq. (1)), the crystallinity index of the regenerated celluloses and the nanocelluloses treated by DHPM and HPH was 57.34%, 40.93%, and 33.57%, respectively. The crystallinity index decreased for the two kinds of nanocelluloses treated with DHPM and HPH because there were more amorphous regions. But crystallinity index of nanocelluloses treated by DHPM was higher than the one treated by HPH because less degraded celluloses entered the clay galleries, resulting in less amorphous region (Cerruti et al., 2008). It suggested that shorter processing time and fewer operating cycles prevented celluloses from being degraded in the DHPM process.

3.2.3. Molecular structural analysis

XPS measurements were performed to investigate the surface chemistry of the regenerated celluloses and the nanocelluloses treated by DHPM and HPH. The O/C atomic ratio of the three samples is shown in Table 1. The O/C atomic ratio of nanocelluloses treated by DHPM was the lowest, indicating that the least amount of carbon atoms had been oxidized. Therefore, celluloses encountered a degradation during the DHPM process at a lower homogenizing frequency and a shorter time, preventing the oxidization of the celluloses.

Table 1
XPS analysis of regenerated celluloses and nanocelluloses treated with DHPM and HPH in the C 1s2s binding energy (B.E.) region.

Samples	O/C	C 1s2; at. %	
		Binding energies	Peak area (%)
Regenerated celluloses	0.59	286.54	9.74
Nanocelluloses treated with DHPM	0.56	286.42	27.89
Nanocelluloses treated with HPH	0.66	285.95	22.16

The C 1s peak is deconvoluted into three sub-peaks, C 1s1, C 1s2, and C 1s3. The one with remarkable change in relative content is C 1s2 (Table 1), which represents single carbon bound to oxygen, i.e. a hydrogen-type species (Topalovic, Nierstrasz, Bautista, Jocic, Navarro & Warmoeskerken, 2007). The contribution of the C 1s2 component in nanocelluloses treated by DHPM is higher than the one treated by HPH. This suggested that there were more hydrogen bonds among cellulose molecules, resulting in a good dispersion and low aggregation by mutual hydrogen bond repulsion interaction (Floury, Desrumaux, Axelos, & Legrand, 2002). Therefore, the dispersion in nanocelluloses fabricated by DHPM is better than the one treated by HPH because of the higher number of exposed hydrogen bonds.

Fig. 4 shows the FT-IR spectra of the regenerated celluloses and nanocelluloses treated by DHPM and HPH. The peak associated with hydrogen bonds is 3383 cm^{-1} for regenerated celluloses, while the peak for nanocelluloses treated by DHPM and HPH moved to the red shift, which were 3444 cm^{-1} and 3439 cm^{-1}, respectively. It suggested that the interchain and intrachain hydrogen bonds between cellulose chains became weaker during DHPM process (Watanabe, Morita, & Ozaki, 2007), compared with the HPH process. It is also in agreement with the XPS analysis.

The peak at 1428 cm^{-1} in the regenerated celluloses is assigned to the intra-molecular hydrogen bonds involved in the O(2)H–O(6) (Hinterstoisser et al., 2003; Zhang & Lynd, 2005; Zhang, Wu, Zhang, & He, 2005). The nanocelluloses treated by DHPM and HPH were shifted to a higher wavenumber, which were 1442 cm^{-1} and 1439 cm^{-1}, respectively. It indicated that the number of intra-molecular hydrogen bonds(O(2)H–O(6)) of nanocelluloses treated by DHPM and HPH decreased. And this also suggested that intra-molecular hydrogen bonds were hardly destroyed by the anions of ionic liquids due to the sudden high pressure and interaction of all kinds of forces coming from the process of DHPM. Therefore, celluloses could avoid degradation, and be kept in its original structure.

The solid-state CP-MAS ^{13}C NMR spectra of the regenerated celluloses and nanocelluloses treated by DHPM and HPH were given in Fig. 5. The chemical shifts of carbon in two kinds of celluloses can be assigned to: 105.2–104.8 ppm for C1; 83.5–87.8 ppm for C4; 74.6–75.0 ppm for C2, C3, C5, and 62.4–62.9 ppm for C6 (Zhang, Dong, & Gao, 2002).

The ^{13}C signal for the C4 is assigned to O(3)H–O(5) intra-molecular hydrogen bonds. For C6, it is assigned to O(2)H–O(6) intra-molecular hydrogen bonds. As shown in Fig. 5, the C4 and C6 peaks of the nanocelluloses treated by DHPM and HPH were shifted to a higher magnetic field. However, disconnected intra-molecular

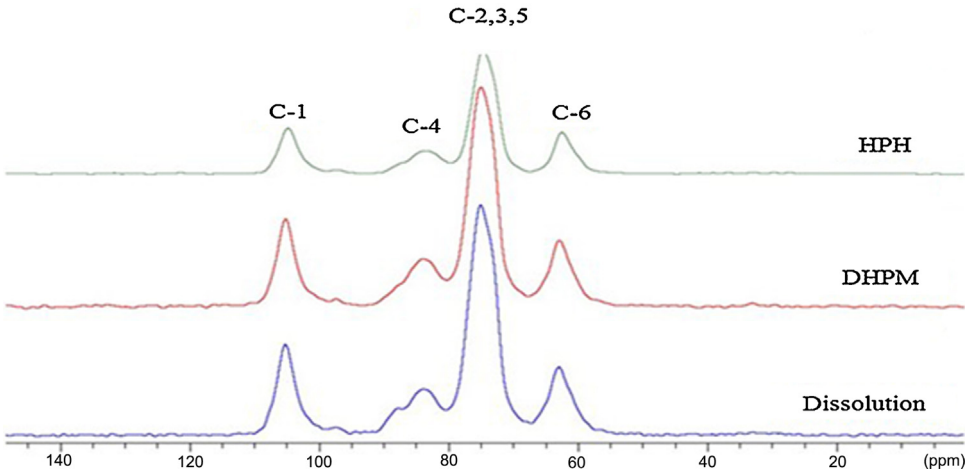

Fig. 5. Comparison of ^{13}C chemical shifts of regenerated celluloses and nanocelluloses treated with DHPM and HPH.

hydrogen bonds (O(2)H–O(6)) and (O(3)H–O(5)) of nanocelluloses treated by DHPM were less than the ones by HPH, which is consistent with the results of FT-IR measurements.

To produce high quality nanocelluloses, it is necessary to investigate the weight-average molecular weight of celluloses. From the experimental results, the weight-average molecular weight of nanocelluloses treated by DHPM was 320,353 Da, while the one by HPH was only 247,730 Da. This suggests that the degree of cellulose degradation in DHPM is lower than the one in HPH, which is attributive to the low influence of less operating cycles and short processing time on intra-molecular hydrogen bonds between cellulose chains. Furthermore, this is supported by the observations resulted from FT-IR and CP-MAS ^{13}C NMR measurements.

3.3. Thermal stability

Fig. 6 shows the TG and DTG curves of the samples. The initial decomposition temperature of the regenerated celluloses and nanocelluloses treated by HPH and DHPM was 317.4 °C, 308.8 °C and 271.8 °C, respectively. Nanocelluloses treated by DHPM exhibited the lowest thermal stability due to its small and uniform particle size, and high surface to volume ratio (Schilling, Bouchard, Khanjian, Phenix, & Rivenc, 2010). This low thermal stability of nanocelluloses could significantly broaden its applications as the nanocellulose process can be operated at a lower temperature (Muhammad et al., 2012).

3.4. Mechanism analysis

Using the homogeneous isolation of nanocelluloses by dynamic high pressure microfluidization, the particle size and conformational characteristics of the celluloses will be changed. Entangled network structures of celluloses were first dispersed in microenvironment, and then hydrogen bonds are weakened by the anions of ionic liquids (Swatloski et al., 2002). Cellulose chains were fractured not only by the shearing forces from high pressure homogenization process pumps, but also by all kinds of other forces, including ultra-high pressure, high-velocity impact, high-frequency vibration, instantaneous pressure drop, intense shear, and turbulence and/or cavitations (Liu, Sale, Simmons, & Singh, 2011) from the collision chamber. Mutual influence of two modes of interaction to celluloses is stronger than the single interaction in HPH process, damaging the intermolecular and intra-molecular hydrogen bonds. As the broken molecular chains turned into smaller pieces, the particle size of the celluloses becomes smaller and nanocelluloses are thus produced. Because of the highly exposed hydrogen bonds on molecular chains, the nanocelluloses are well dispersed, which prevents the aggregation from the repulsion interaction of mutual hydrogen bonds. Furthermore, because of the high pressure and high stress of head-on collision (Keerati & Corredig, 2009), the process needs a very short time. Consequently, intra-molecular hydrogen bonds are hardly destroyed by the anions of ionic liquids, and the degradation and destruction on the structure of celluloses are thus avoided. Therefore, the DHPM process can produce

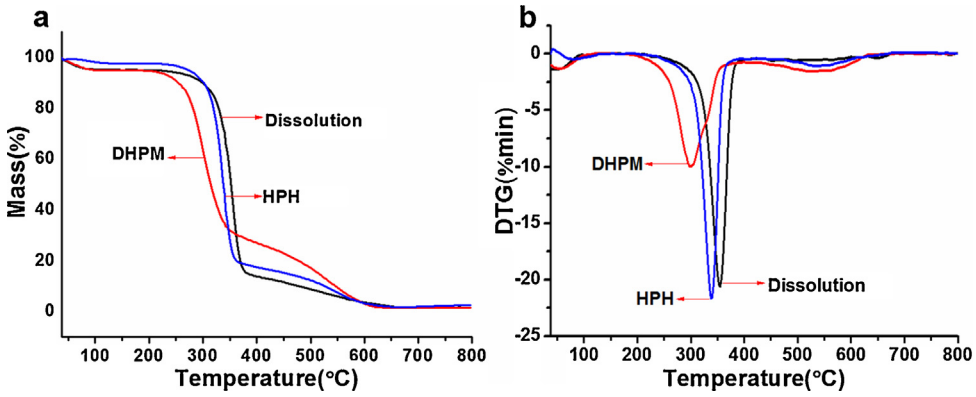

Fig. 6. TG and DTG curves of regenerated celluloses and nanocelluloses treated with DHPM and HPH.

nanocelluloses with small particle size and a narrow dispersion. It can also maintain the original properties for many potential applications, such as medicine, packaging, electronics and printing.

4. Conclusion

In the present work, nanocelluloses were produced through dynamic high pressure microfluidization by precisely controlling the shearing force and pressure in microenvironment. The nanocelluloses treated by DHPM had a diameter varying from 5 nm to 12 nm and a narrower size distribution than the one treated by HPH, which could be due to the intermolecular hydrogen bonds of the celluloses were easier to be broken in the DHPM process through FT-IR, XPS, CP/MAS ^{13}C NMR, GPC and rheological properties analysis. However, the DHPM process has little impact on the intra-molecular hydrogen bonds due to short process time. This could prevent the degradation and destruction on the cellulose structures. Applications of these nanocelluloses will be explored in the future.

Acknowledgments

This work was financially supported by the Fundamental Scientific Research Funds for Chinese Academy of Tropical Agricultural Sciences (1630062013012) and the special operating expenses from Chinese National Engineering Research Center building program (2011FU125Z09). The work is also partially supported by Chinese Central Government 948 Research program (2012-Z10), and Major Science and Technology Projects of Hainan Province (ZDZX2013023-3).

References

Adsul, M., Soni, S. K., Bhargava, S. K., & Bansal, V. (2012). Facile approach for the dispersion of regenerated cellulose in aqueous system in the form of nanoparticles. *Biomacromolecules*, *13*(9), 2890–2895.

Cerruti, P., Ambrogi, V., Postiglione, A., Rychlyí, J., Matisovaí-Rychlaí, L., & Carfagna, C. (2008). Morphological and thermal properties of cellulose-montmorillonite nanocomposites. *Biomacromolecules*, *9*, 3004–3013.

Collier, J. R., Watson, J. L., Collier, B. J., & Petrovan, S. (2009). Rheology of 1-butyl-3-methylimidazolium chloride cellulose solutions. II. Solution character and preparation. *Journal of Applied Polymer Science*, *111*, 1019–1027.

Floury, J., Desrumaux, A., Axelos, M. A. V., & Legrand, J. (2002). Degradation of methylcellulose during ultra-high pressure homogenization. *Food Hydrocolloids*, *16*, 47–53.

Hinterstoisser, B., Åkerholm, M., & Salmeín, L. (2003). Load distribution in native cellulose. *Biomacromolecules*, *4*(5), 1232–1237.

Hu, X., Zhao, M., Sun, W., Zhao, G., & Ren, J. (2011). Effects of microfluidization treatment and transglutaminase cross-linking on physicochemical, functional, and conformational properties of peanut protein isolate. *Journal of Agricultural and Food Chemistry*, *59*(16), 8886–8894.

Ikeda, T., Holtman, K., Kadla, J. F., Chang H.-m., & Jameel, H. (2002). Studies on the effect of ball milling on lignin structure using a modified method. *Agricultural and Food Chemisity*, *50*, 129–135.

Keerati, U. R. M., & Corredig, M. (2009). Effect of dynamic high pressure homogenization on the aggregation state of soy protein. *Journal of Agricultural and Food Chemistry*, *57*(9), 3556–3562.

Klemm, D., Heublein, B., Fink, H.-P., & Bohn, A. (2005). Cellulose: Fascinating biopolymer and sustainable raw material. *Angewandte Chemie International Edition*, *44*(22), 3358–3393.

Lavoine, N., Desloges, I., Dufresne, A., & Bras, J. (2012). Microfibrillated cellulose – Its barrier properties and applications in cellulosic materials: A review. *Carbohydrate Polymers*, *90*(2), 735–764.

Li, J., Wei, X., Wang, Q., Chen, J., Chang, G., Kong, L., et al. (2012). Homogeneous isolation of nanocellulose from sugarcane bagasse by high pressure homogenization. *Carbohydrate Polymers*, *90*(4), 1609–1613.

Liu, H., Sale, K. L., Simmons, B. A., & Singh, S. (2011). Molecular dynamics study of polysaccharides in binary solvent mixtures of an ionic liquid and water. *The Journal of Physical Chemistry B*, *115*(34), 10251–10258.

Martínez, J. M., Reguant, J., Montero, M. Ä., Montaneí, D., Salvadoí, J., & Farriol, X. (1997). Hydrolytic pretreatment of softwood and almond shells. Degree of polymerization and enzymatic digestibility of the cellulose fraction. *Industrial & Engineering Chemistry Research*, *36*, 688–696.

Muhammad, N., Omar, W. N., Man, Z., Bustam, M. A., Rafiq, S., & Uemura, Y. (2012). Effect of ionic liquid treatment on pyrolysis products from bamboo. *Industrial & Engineering Chemistry Research*, *51*(5), 2280–2289.

Pereda, J., Perragut, V., Quevedo, J. M., Guamis, B., & Trujillo, A. J. (2008). Effects of ultra-high-pressure homogenization treatment on the lipolysis and lipid oxidation of milk during refrigerated storage. *Journal of Agricultural and Food Chemistry*, *56*, 7125–7130.

Sasaki, M., Adschiri, T., & Araai, K. (2003). Production of cellulose II from native cellulose by near- and supercritical water solubilization. *Journal of Agricultural and Food Chemistry*, *51*, 5376–5381.

Schilling, M., Bouchard, M., Khanjian, H., Phenix, T. L. A., & Rivenc, R. (2010). Application of chemical and thermal analysis methods for studying cellulose ester plastics. *Accounts of Chemical Research*, *43*, 888–896.

Swatloski, R. P., Spear, S. K., Holbrey, J. D., & Rogers, R. D. (2002). Dissolution of cellose with ionic liquids. *Journal of American Chemical Society*, *124*(18), 4974–4975.

Topalovic, T., Nierstrasz, V. A., Bautista, L., Jocic, D., Navarro, A., & Warmoeskerken, M. M. C. G. (2007). XPS and contact angle study of cotton surface oxidation by catalytic bleaching. *Colloids and Surfaces A: Physicochem. Eng. Aspect*, *296*, 76–85.

Watanabe, A., Morita, S., & Ozaki, Y. (2007). Temperature-dependent changes in hydrogen bonds in cellulose Iα studied by infrared spectroscopy in combination with perturbation-correlation moving-window two dimensional correlation spectroscopy: Comparison with cellulose I. *Biomacromolecules*, *8*(9), 2969–2975.

Weng, L., Zhang, L., Ruan, D., Shi, L., & Xu, J. (2004). Thermal gelation of cellulose in a NaOH/Thiourea aqueous solution. *Langmuir*, *20*, 2086–2093.

Yue, Y., Zhou, C., French, A. D., Xia, G., Han, G., Wang, Q., et al. (2012). Comparative properties of cellulose nano-crystals from native and mercerized cotton fibers. *Cellulose*, *19*, 1173–1187.

Zhang, H., Wu, J., Zhang, J., & He, J. (2005). 1-allyl-3-methylimidazolium chloride room temperature ionic liquid:a new and powerful nonderivatizing solvent for cellulose. *Macromolecules*, *38*, 8272–8277.

Zhang, L., Ruan, D., & Zhou, J. (2001). Structure and properties of regenerated cellulose films prepared from cotton linters in NaOH/Urea aqueous solution. *Industrial & Engineering Chemistry Research*, *40*, 5923–5928.

Zhang, L., Dong, R., & Gao, S. (2002). Dissolution and regeneration of cellulose in NaOH/thiourea aqueous solution. *Journal of Polymer Science Part B: Polymer Physics*, *40*(14), 1521–1529.

Zhang, Y.-H. P., & Lynd, L. R. (2005). Determination of the number-average degree of polymerization of cellodextrins and cellulose with application to enzymatic hydrolysis. *Biomacromolecules*, *6*, 1510–1515.